This is the Pre-Published Version.

This version of the article has been accepted for publication, after peer review (when applicable) and is subject to Springer Nature's AM terms of use(https://www.springernature.com/gp/open-research/policies/accepted-manuscript-terms), but is not the Version of Record and does not reflect post-acceptance improvements, or any corrections. The Version of Record is available online at: https://doi.org/10.1007/s40843-020-1595-2.

Low-carbon advanced nanostructured steels: Microstructure, mechanical properties, and applications

Haojie Kong[1], Zengbao Jiao[2], Jian Lu[1,4,5] and Chain Tsuan Liu[1,3,4,5*]

[1] Department of Mechanical Engineering, City University of Hong Kong, Hong Kong, China

[2] Department of Mechanical Engineering & Shenzhen Research Institute, The Hong Kong Polytechnic University, Hong Kong, China

[3] Department of Materials Science and Engineering, City University of Hong Kong, Hong Kong, China

[4] Center for Advanced Structural Materials, Department of Mechanical Engineering, City University of Hong Kong, Hong Kong, China

[5] Hong Kong Institute for Advanced Study, City University of Hong Kong, Hong Kong, China

[*] Corresponding author (email: chainliu@cityu.edu.hk)

Abstract

Low-carbon advanced nanostructured steels have been developed for various structural engineering applications, including bridges, automobiles, and other strength-critical applications such as the reactor pressure vessels in nuclear power stations. The mechanical performances and applications of these steels are strongly dependent on their microstructural features. By controlling the size, number density, distribution, and types of precipitates, it is possible to produce nanostructured steels with a tensile strength reaching as high as 2GPa while keeping a decent tensile elongation above 10% and a reduction of area as high as 40%. Besides, through a careful control of strength contributions from multiple strengthening mechanisms, the nanostructured steels with superior strengths and low-temperature impact toughness can be obtained by avoiding the temper embrittlement regime. With appropriate Mn additions, these nanostructured steels can achieve a triple enhancement in ductility (total tensile elongation, TE of ~30%) at no expense of strengths (yield strength, YS of ~1100 to 1300 MPa, ultimate tensile strength, UTS of

~1300 to 1400MPa). More importantly, these steels demonstrate good fabricability and weldability. In this paper, the microstructure-property relationships of these advanced nanostructured steels are comprehensively reviewed. In addition, the current limitations and future development of these nanostructured steels are carefully discussed and outlined.

Keywords: heterogeneous, nano-precipitates, strength-ductility paradox, embrittlement, dislocation interactions

INTRODUCTION

Nanostructured steels are generically referred as high-strength steels with nanometer-scale structures. According to Bhadeshia[1], the term 'nanostructures' carries a more stringent meaning and is defined as nano-scale features with a large interfacial area to volume ratio (S_v) over 0.04nm^{-1}. The conventional nanostructured steels usually have ultra-fine grains and low uniform tensile elongations[2]. Large deformation or severe plastic deformation is often required to obtain such ultra-fine grains, complicating the steel manufacturing process, especially in the production of large parts or cast products[3]. Recently, a new class of fully commercialized bainitic nanostructured steels well suited for a large-scale large-part production was successfully developed by Bhadeshia *et al.*[1,4]. However, these steels require a long aging time and are difficult to be welded due to their high carbon content. In this review, we will focus on the recently developed low-carbon advanced nanostructured steels strengthened with a high number density of ultrafine coherent Cu and NiAl precipitates[5–17]. Due to the presence of densely dispersed ultrafine precipitates, these advanced nanostructured steels have a high S_v ratio around 0.03 nm^{-1}, very close to the Bhadeshia's definition. Besides, Liu and co-workers[18] discovered that, through simultaneous Cu and Mn alloying additions

together with simple thermo-mechanical treatments, it is possible to obtain multi-phase ultrafine Cu precipitate-strengthened steels with submicrometer-sized (~300 to 500 nm) grains without complicated processing routes generally required in the conventional ultra-fine grain steels. As depicted in Fig. 1, these nano-precipitate-strengthened advanced nanostructured steels show an excellent strength-ductility balance and outperform the conventional dual phase (DP), transformation induced plasticity (TRIP), and high carbon martensitic (MART) steels[13]. On top of that, these advanced nanostructured steels have superior weldability due to the low level (< 0.15 wt%) carbon additions[19,20]. In spite of their ultrahigh yield strength (YS, ~1 to 2GPa), their tensile reduction area (RA) can reach over 40%, indicating an excellent fabricability. Moreover, they are relatively cheaper (raw material cost) than the traditional high-strength maraging steels containing a high level of expensive elements such as Co and Ti. All these attractive properties allow the advanced low-carbon nanostructured steels to serve in various important structural engineering applications involving transportation, infrastructure, maritime, energy, and defense industries[8,21–24]. These advanced nanostructured steels are normally homo-genized at 900–950℃ and isothermally aged at a relatively lower temperature around 400–550℃ , as depicted in Fig. 2a. In order to produce a complex heterogeneous microstructure consisting of multiple nano-scale phases, multi-step heat treatments presented in Fig. 2b are re- quired. Liu and co-workers [18] have demonstrated that a short annealing at 700℃ can induce a partial re crystallization and the formation of submicrometer-sized (~300 to 500nm) austenite grains that later transform into submicron-martensitic grains during the water quenching of the nanostructured steels containing Cu and Mn additions. The subsequent double-step low-temperature annealing at 640 and 500℃ will stimulate the formation of relatively stable submicrometer-sized (~300 to 500nm) reversed austenite grains along with the precipitation of coherent Cu precipitates (~3 to 4nm) located at grain

boundaries. This complex heterogeneous microstructure results in better dislocation accumulation mechanisms that bring an enhanced strength-ductility balance and will be further elaborated in the text later. Raising the homogenization temperature to above 900℃ can help improve strengths due to enhanced supersaturation[9]. However, a care should be taken as performing homogenization at too high temperatures, such as above 1050℃, which can lead to steel softening due to an excessive grain growth. Homogenization at above 1250℃ can also encourage the formation of Widmanstaten ferrite and deteriorate the impact toughness [25]. Another feasible processing route of the advanced nanostructured steels involves interphase precipitation during the continuous cooling from the 900℃ homo-genization, as shown in Fig. 2c, particularly useful for as- cast products [26]. The process parameters and compo- sitions of some recently developed low-carbon nano- precipitate-strengthened advanced nanostructured steels are also tabulated in Table 1.

TOWARDS THE GIGAPASCAL GRADE NANO-PRECIPITATE-STRENGTHENED LOW-CARBON DUCTILE ADVANCED NANOSTRUCTURED STEELS

With the recent rapid growth of the world population and the global quest to reduce the carbon dioxide emission, new cheap weldable advanced nanostructured steels with an ultra-high-strength (YS >1 GPa), satisfactory tough- ness (tensile elongation >10%; impact toughness >200 J at −40°C), and good fabricability (area reduction >60%) are critically needed. The achievement of such ultra-high- strength improvement in the low-carbon advanced nano- structured steels without a loss of ductility through the dense dispersion of ultrafine nano-scale precipitates is of great technological importance. Just by increasing the use of high-strength steels by 35%, the carbon emission can be cut down by at least 70% [27]. However, the conven- tional high-strength steels contain a high level of

carbon, making these steels difficult to weld. The weldability of a steel is very important in the real-world application. For instance, the welding work can contribute to about 30% of the total cost in ship building [28].

Recently, Huang's group [29,30] successfully developed an ultra-high-strength steel of YS ~2.2GPa along with a superb tensile uniform elongation of ~16% and fracture toughness (K_{JIC}~102MPa $m^{0.5}$). However, the steel has a serious welding issue due to a very high level of carbon (0.47 wt%). Moreover, this steel requires a processing step involving an extensive plastic deformation during the manufacturing, thus limiting their use in as-cast products. On the other hand, the nano-precipitate-strengthened high-strength steel (YS ~1.4GPa and uniform tensile elongation ~7%) developed by Raabe *et al*. [31] contains a very minimal level (~0.01 wt%) of carbon. Due to the low level of carbon, the steel has good weldability. Never-theless, the tensile strengths and uniform elongation are only half of that of Huang's ultra-high-strength steel. At any rate, both these two steels contain a high level of Mn (~10–12 wt%). Mn can vaporize easily during steel smelting and is disfavoured by the steel industry.

The roles of alloying additions

The low-carbon advanced nanostructured steels are composed of a complex chemistry with various alloying additions, as summarized in Table 1. The three elements of Cu, Ni, and Al are added primarily to form Cu-rich and NiAl precipitates due to their reduced solubility limit or the presence of a miscibility gap in the body-centered cubic (BCC) Fe matrix as temperature decreases [5,32]. In order to obtain highly dispersed coherent Cu-rich nanoscale precipitates, Ni additions are essential to reduce the energy barrier of nucleation by lowering the interfacial energy as well as the elastic misfit

strain energy [5]. On the other hand, Mn additions are required for a dense dispersion of coherent NiAl precipitates [7]. Mo additions were also reported to increase the nucleation density of NiAl precipitates by reducing the lattice misfit at the precipitate-matrix interface, apart from slowing the coarsening kinetics of the precipitates [8]. The additions of Mn are also beneficial for stabilizing the austenite phase that permits the martensite formation in the subsequent quenching or deformation, which is important for the development of strong yet ductile nanostructured steels [18]. The complex interactions among the alloying additions are further elaborated in the section of "NANOSCALE Cu AND NiAl PRECIPITATIONS IN NANOSTRUCTURED STEELS".

Cu-rich nano-precipitate strengthening

Cu-rich precipitation has been used in the high-strength low-alloy (HSLA) steel series since about a decade ago, for replacing the high yield (HY) steel which is difficult to weld. This HSLA steel series contain overaged Cu-rich precipitates with its YS in the range of 550–850 MPa.

Enormous efforts have been put forth by several research groups to maximize the strength of these nanostructured steels hardened by the Cu-rich precipitation. Fine's group[33] from the Northwestern University started off by removing the Mo and Cr from the steel chemistry to reduce the hardenability and thus producing ferritic steels fully strengthened by Cu-rich precipitates (NuCu 60 and NuCu 70). These steels contain Cu, Ni, Mn, and C additions of 1.3–1.4, 0.5–0.85, 0.5–0.8, and 0.03–0.06 wt%, respectively. The steel billets were homogenized at 1093℃, hot rolled to 12.2-mm-thick plates with a finish rolling temperature of 871℃, and then air cooled to room temperature [34]. With this thermal history, these steels can achieve YS of 400–500 MPa, tensile elongation of 27%–36%, and impact toughness of >136 J at −40℃ [33,35]. The low YS of these steels are believed to

be attributed to the relatively thick specimens and slow cooling rates that result in growth and coarsening of Cu-rich precipitates [25,36]. The steels were used for the construction of a bridge in Lake Villa, Illinois in 2005 [37]. In the steel manufacturing, steel sheets are normally coiled up to facilitate storage and transport process. The coiled steels are then uncoiled for the subsequent treatments before obtaining the final products. Steels with a low YS during the uncoiling stage but with an increased strength for meeting the require- ments of a product at the final stage are often desirable. Precipitation strengthening is one of the good ap- proaches. For example, the ferritic NuCu 60 and NuCu 70 steels have a low YS (~400–500 MPa) in the as-hot-rolled state. These steels can achieve a higher YS (~700 MPa) easily by a simple 900°C water quenching with a sub- sequent isothermal aging at 525℃ for 1 h [33,35].

A few years later, a low-carbon advanced nano-structured steel named NuCu 140 with even a higher YS reaching 965 MPa, targeting for the explosion resistant steel application, was developed for United State Navy [35]. It was produced by 900℃ water quenching and a subsequent heat treatment at 550℃ for 2 h to acquire a high number density (order of magnitude approaching $10^{24}m^{-3}$) of ultrafine 3 nm coherent Cu-rich precipitates homogeneously dispersed in the ferritic matrix [35]. Different from NuCu 60 and NuCu 70, NuCu 140 con- tains minor Al additions of 0.69 wt% and a substantially higher Ni percentage of 2.87 wt% [35]. NuCu 170, a ferritic advanced nanostructured steel with YS approaching 1200 MPa, was also produced by increasing the Ni and Cu content to 2.83 and 2.09 wt%, respectively [10,21,38]. On the other hand, Jiao *et al.* [5] discovered the synergistic effects of Ni additions on the nucleation of Cu-rich precipitates. They successfully developed a low- carbon ferritic advanced nanostructured steel (Cu/Ni steel) that achieved the YS of 1042 MPa while keeping a satisfactory uniform tensile elongation of 10% (the area reduction over 60%) with only a minimal

Ni content. Ni additions of 0.75 to 2 wt% of Cu were sufficient to yield a high number density (7×10^{23} m^{-3}) of ultrafine (3 nm) coherent BCC Cu precipitates, as depicted in Fig.3. This is an important discovery as it implies a significant cost reduction due to only a minimal Ni addition which is required to induce a significant strength improvement (437 MPa) at a very minimal cost of ductility. The grain size reduction due to the reduced austenite to ferrite transformation temperature as a result of Ni and Cu additions also contributes to an additional strengthening and ductility. The reduced grain size allows the activation of more slip systems, leading to a more homogenized slip distribution and therefore an improved ductility The high area reduction (~60%) suggests that Jiao and Liu's Cu-rich nano-precipitate-strengthened advanced nanostructured steel possesses a high workability and is well suited for applications that require a large cold work, such as the anti-roll bars for maintaining the stability of a vehicle during fast cornering[40]. A recent breakthrough in the strength-ductility paradox with a triple ductility enhancement (uniform tensile elongation ~27%) at no expense of strengths (YS ~1100 MPa and ultimate tensile strength (UTS) ~1300 MPa) through combined Cu and Mn additions with simple low-temperature double-step heat treatments was reported by Liu's group [18]. The additions of Mn have been found to be effective in improving the ductility of these steels. Bhadeshia [41] pointed out that the large ductility of Mn steels does not seem rely solely on the TRIP but most probably due to the resultant complex deformation behavior of different phases. Raabe and co-workers [42] believe that the large ductility is attributed to the austenite grains with different stabilities which contribute to a large deformation regime. Based on the work by Liu's group [18], the combined Cu and Mn additions encourage the formation of stable and hard submicrometer-sized (~300 to 500nm) reversed austenite grains along with nanoscale coherent Cu precipitates located at grain boundaries, as demonstrated in Fig. 4e. These relatively hard submicrometer-sized (~300 to 500 nm)

reversed austenite grains, in addition to the dislocations pinning by the coherent Cu precipitates, contribute to the strength of the steel. Meanwhile, the ductility arises from the synergistic effects of Cu precipitates in stabilizing the austenite grains that result in a more gradual release of stress through progressive TRIP as well as creating a more heterogeneous strain parti-tioning [43–47]. The strain partitioning leads to an enhanced dislocation accumulation and work hardening due the formation of stress-strain gradients as a result of the pile-up of geometrical necessary dislocations near the grain boundaries and the generation of long-range back stresses [48,49]. The coherent Cu precipitates at the grain boundaries also strengthen the grain boundaries by promoting a better stress-strain transfer and avoiding the stress-strain localization as a consequence of grainboundary dislocation thickening [44,46]. A microstructure with gradient structures [50,51] and a mini- mized strain contrast [52,53] among the adjacent phases is effective in suppressing the stress-strain localization, resulting in an enhanced strength-ductility synergy.

NiAl nano-precipitate strengthening

In order to develop advanced nanostructured steels with even a higher strength, researchers[7,8,54] started to borrow the idea from the maraging steels and derive strength from intermetallic compounds [55–60]. NiAl is an intermetallic compound and incorporating it in steels can lead to serious brittleness [54,61–63]. Jiao *et al.* [7] successfully turned brittleness into ductility and developed an advanced nanostructured steel alloy (Fe-5Ni-1Al-3Mn, wt%) strengthened by a high number density of ultrafine coherent NiAl precipitates. This advanced nanostructured steel alloy is carbon free. With a simple heat treatment at 550 ℃ for 2h preceded by a water quenching from the 900 ℃ 30-min homogenization, it can achieve a strength (YS = 1225 MPa) comparable to the PH 13-8 type

maraging steel (YS = 1200 MPa) with almost no loss of tensile ductility, as depicted in Fig.5. The tensile ductility and RA can be maintained at 14% and over 50%, respectively. For the steel to be cost competitive, Jiao *et al*.[7] kept the Ni content at only 5 wt%, lower than that of the PH 13-8 maraging steel (~8 wt% of Ni). They discovered that Mn additions are very important as Mn is cheap and, more importantly, the number density of NiAl precipitates is increased by at least 50 times, from the order of ~10^{22} to ~10^{24} m^{-3} and at the same time reducing the size of the precipitates to 2.8 nm in diameter, resulting in a three-fold strength increment by 540 MPa. The NiAl precipitates in Jiao and Liu's Fe-5Ni-1Al-3Mn na- nostructured steel [7] and the Cu-rich precipitates in Jiao and Liu's Cu/Ni nanostructured steel[5] have the similar size and number density, yet the strength increment due to the NiAl precipitation (540MPa) is higher than that of the Cu precipitates (437MPa). This suggests that nanoscale NiAl precipitates are harder and have a higher intrinsic strength. The beneficial effects of Mn additions are attributed to the substitution of Al sublattice by the Mn atoms, reducing the critical energy formation of NiAl precipitates.

Jiang *et al*.[8] also reported an unusual behavior of an advanced nanostructured steel strengthened by a dispersion of a high number density (over 3.7 × 10^{24} m^{-3}) of ultrafine (~2.7nm in diameter) coherent NiAl precipitates with minimal lattice misfit (~0.03%) in a martensitic matrix. Jiang and Lu's steel has an elemental composition very similar to the grade 350 or 18 Ni maraging steel but with the replacement of expensive Co (~11 wt%) and Ti (~1.5 wt%) with Al (3 wt%) which is cheaper. With this new chemistry, their new steel does not rely on the strengthening from the Ni_3Ti and Ni_3Mo precipitates as in the traditional 350 maraging steel. This saves more Ni atoms for the steel matrix, creating a higher supersaturation or driving force for nucleation and thus finer and higher number density NiAl precipitates. After the 900°C solutionization for 15 min followed with a 500°C aging

for 3 h, this advanced nanostructured steel can achieve a tensile YS over 2 GPa. The strength-ducti-lity paradox is a common scenario for almost all materials. Nevertheless, as described in Fig. 6, Jiang and Lu's steel behaves very unusually in the sense that the tensile uniform elongation increases from 1.9% to 3.8% as the YS increases from 900 MPa to 2 GPa upon the 500°C treatment. In other words, the dispersion of a high number density of ultrafine coherent precipitates in steels can serve as effective barriers for dislocation motion and at the same time delaying the initiation of necking instability, breaking the common notion of strength-duc-tility paradox. This is an important discovery as real engineering applications require both the strength and ductility.

On the other hand, Liaw's group focused on the development of low-cost advanced nanostructured steels for steam turbine applications. The conventional NiAl precipitate-strengthened maraging steels such as PH 13-8 have intermediate service temperatures below 600°C, due to the low volume fraction (~3%) of NiAl precipitates [32,55] and low reversed austenite temperature (<600°C) [55,64–68]. Liaw's group [62,69] developed a nanostructured ferritic steel (FBB-8: Fe-6.5Al-10Cr-10Ni-3.4Mo-0.25Zr-0.005B, wt%) with a high-volume fraction (~16%) of NiAl precipitates. A high-volume fraction of NiAl precipitates is crucial for enhanced creep resistance but often results in poor room temperature ductility (bending ductility <2%) [63,70]. The NiAl precipitates in the FBB-8 steel are of duplex-type: large (~100 nm in diameter) primary and ultrafine (~3 nm in diameter) secondary nanoscale NiAl precipitates. These precipitates are coherent with the ferritic matrix with a near-zero lattice misfit (0.06% for the primary precipitates), for a low driving force for coarsening [54,62,71]. Compared with the Jiao and Liu's [7] and Jiang and Lu's [8] nanostructured steels, Liaw's FBB-8 steel has the highest volume fraction of NiAl precipitates. The precipitate-dis-tribution parameters including the volume fraction, size and number density of the NiAl precipitates of these steels are

listed in Table 2. Moreover, Liaw's group fixed the Al:Ni ratio of the FBB-8 steel at 0.65, the highest among Jiao and Liu's (Al:Ni = 0.2 [7]), Jiang and Lu's (Al: Ni = 0.17 [8]) and PH 13-8 (Al:Ni = 0.09 [55]) steels. A low Al:Ni ratio reduces the austenite reverse temperature, leading to a significant strength reduction at the elevated temperatures and thus restricting the steels to only serve in the intermediate temperature environment with operating temperatures below 600°C [55,64–68]. In spite of the increased NiAl volume fraction and austenite reversed temperature, the creep resistance of the FBB-8 steel is still not sufficient for the industrial steam turbine applications above 700°C [69], most probably due to the dissolution of the ultrafine secondary NiAl precipitates at elevated temperatures [62]. In addition, the lack of a load transfer from the steel matrix to the primary NiAl precipitates attributed from the diffusional flow along the NiAl/matrix can also result in the poor creep resistance [69]. Song *et al.* [69] improved the creep resistance of the steel by adding 2 wt% of Ti to create hierarchical structured B2-NiAl/$L2_1$-Ni_2TiAl precipitates, as shown in Fig. 7. These hierarchical structured precipitates have a strong coherent misfit strain along the matrix/precipitate interface, and they are effective obstacles against the dislocation climb-bypassing or shearing. The modified steel has a creep resistance comparable to the Haynes 282 Ni-based superalloys and is well suited for applications up to 760°C for ultra-supercritical steam turbines.

Co-nano precipitate strengthening

Though NiAl precipitates are more effective strengtheners than the Cu precipitates, in many applications where cost is concerned, deriving strength solely from the expensive NiAl precipitates might not be favorable. Many researchers [6,9,11] showed their interest in the steels containing multiple components such as Cu, Ni, Al, Mn. Zhang et al. [11] investigated the effects of Ni on a ferritic

multicomponent alloy system (Fe-1.2Al-1.5Mn-2.87Cu, wt%) and developed a nanostructured steel strengthened with a high number density ($3.6 \times 10^{24}\ m^{-3}$) of ultrafine (diameter ~3 nm) NiAl and Cu co-precipitates. The au- thors discovered that the additions of 4 wt% Ni to the steel were able to increase the YS from about 700 MPa in the solution state to approximately 1.4 GPa upon aging, a significant strength increment of nearly 700 MPa with no significant loss of ductility. The total tensile elongation could be still maintained at ~16%. Later, Xu *et al.* [14] demonstrated that the total elongation can be further improved by nearly twice, to approximately 30%, after the additions of 9 wt% of Mn. The YS was slightly reduced to 1.3 GPa while the UTS was maintained at about 1.4 GPa. The authors attributed the improved tensile ductility to the cooperative deformation of the soft austenite grains and the adjacent hard tempered martensite grains strengthened mainly by the high number density ($\sim 1 \times 10^{24}\ m^{-3}$) of ultrafine (~3.5 nm) Cu and NiAl precipitates. The cooperative deformation triggers the activation of multiple slip systems and suppresses the strain localiza- tion as a result of the dynamic stress-strain partitioning and TRIP effect.

Kapoor *et al.* [9] further increased the strengths of the co-precipitate-strengthened ferritic steel (Fe-3Cu-4Ni-1.5Al-3Mn-0.07Nb-0.53Si-0.05C, wt%) to 1.6 GPa with about 4% of total tensile elongation by increasing the total concentration of the principal elements (Mn+Ni+Cu+Al) to 11.5wt%. Increasing the concentration of principal elements can result in two competing consequences. First, the driving force and the volume fraction of the Cu and NiAl precipitates will increase, leading to enhanced strength. Secondly, the principal elements Mn, Ni, and Cu are austenite stabilizers. The increase of these element concentrations will also increase the concentration of austenite stabilizers. As the principal element concentra- tion goes beyond 11.5wt%, austenite will easily form during aging; as a result, the steel becomes soft and its YS decreases.

Through computation-aided alloy design strategy, Jiao *et al.*[6] successfully developed a Cu-rich and NiAl coprecipitate-strengthened advanced nanostructured steel (Fe-1.5 Cu-5 Ni-2 Al-3 Mn-1.5Mo-1.5W-0.07Nb-0.01B-0.05C, wt%) containing a low-carbon content with a UTS close to 2 GPa while keeping the total tensile elongation at ~10%. By optimizing the alloying content, the tensile strength (YS ~1.7 GPa, UTS ~1.9 GPa) of this advanced nanostructured steel is only a few hundred MPa below Jiang and Lu's steel [8] (YS ~2 GPa, UTS ~2.2 GPa), yet the cost is relatively cheaper. According to the market price [72,73], Ni is about 45 times more expensive than Fe. This new steel keeps the expensive Ni content at a very minimal level of only 5 wt%, compared with the 18 wt% of Ni content in the Jiang and Lu's steel, lowering the steel material cost by almost 64%. Moreover, it is very interesting to note that even though both the Jiao and Liu's and Kapoor and Isheim's co-precipitate-strength- ened steels have the same principal element (Mn+Ni+Cu +Al) concentration or supersaturation for nucleation, Jiao and Liu's steel can reach even higher strengths (YS ~1.7 GPa, UTS ~1.9 GPa). Both the steels were peak aged at 550°C for 2 h. The principal element concentration of Jiao and Liu's steel was optimized so that the austenite volume fraction maintained below 15% with no forma- tion of delta-ferrite was permitted. Different from the Kapoor and Isheim's steel, the Ni:Cu and Al:Cu ratios are relatively higher. The high strengths and improved tensile ductility in Jiao and Liu's steel might be due to the finer and higher number density of NiAl and Cu co-pre-cipitates. The Cu and NiAl precipitates in Jiao and Liu's steel are around 3 nm in diameter, twice finer than that of Kapoor and Isheim's steel. Meanwhile, the number den- sity of Cu and NiAl precipitates in Jiao and Liu's steel are 5×10^{23} and 3×10^{24} m^{-3}, respectively, an order of magnitude higher than that of the Kapoor and Isheim's steel. In addition, the presence of nano-scale carbides and reduced grain size can also contribute to a supplementary strengthening effect.

THE IMPACT TOUGHNESS OF THE NANO-PRECIPITATE-STRENGTHENED LOW-CARBON ADVANCED NANOSTRUCTURED STEELS

Impact toughness is a very important design criterion in many structural applications especially for those invol- ving a low service temperature. It is defined by the minimum energy required for the initiation and propagation of cracks [74]. Ferritic and martensitic steels are susceptible to low-temperature brittleness or embrittle- ment due to their intrinsic temperature-strength dependency. As the temperature reduces, the YS increases [75,76]. Once the temperature drops to below the ductile to brittle transition temperature (DBTT), brittle failure occurs. The sinking of titanic ship is one of the cata- strophic metallurgical failures due to the low temperature embrittlement. According to the Yoffee diagram [77], brittle failure occurs once the YS of a steel exceeds its fracture strength. The diagram also suggests that intergranular fracture is the dominant brittle fracture mode when the intergranular fracture strength is lower than the transgranular fracture strength; otherwise, transgranular cleavage will be the main brittle failure mode. In the conventional martensitic steels, brittle failures involving both cleavage and intergranular fractures can occur after tempering at temperatures around 200–400°C (also called as the irreversible 350°C temper martensite embrittlement) due to the precipitation of brittle carbides along the inter-lath and grain boundaries [75,78]. The reversible intergranular 300–600°C temper embrittlement is another type of brittle failure commonly found in the ferritic/martensitic steels due to the segregation of impurities along the prior austenite grain boundaries [79].

The Cu-rich precipitate-strengthened ferritic steels de- veloped by the Fine's group, such as the NuCu 60 and 70 steels, have a superior impact toughness over 136 J even at a cryogenic temperature of −40°C [33,35]. However, the impact toughness reduces to 74 J (at −40°C) as the YS increases to 956

MPa in the NuCu 140 [35]. A similar strength-impact toughness paradox can also be observed in the Cu precipitate-strengthened HSLA-100 steel, as demonstrated in Fig. 8. The steel achieved its peak strengths after aging at temperatures around 300–600°C but at the expense of impact toughness [80]. The impact toughness restored with increasing aging temperature, but it came with reduced strengths. The reduced impact toughness after aging at 300–600°C was ascribed to the improved matrix strength as a result of the profuse Cu-rich precipitation. The steel regained its toughness with higher aging temperatures due to the coarsening of the Cu-rich precipitates. Similar strength-impact toughness trade-off was also reported in the ferritic/martensitic steels containing Cu-rich precipitates developed by Liu *et al.* [81] from Gu's group. These authors found that the strength improvement due to the Cu-rich precipitation during the 500°C tempering could lead to a reduced impact toughness. Meanwhile, tempering at temperatures above 600°C resulted in improved impact toughness but at the expense of strengths due to the formation of re- versed austenite.

As discussed in the earlier sections, the low-carbon Cu-rich nano-precipitate-strengthened advanced nanostructured steels developed by Jiao *et al.* [5] acquire their strengths obtained from high-number-density ultrafine coherent Cu precipitates. The nanostructured steels require aging at 550°C to obtain the critical precipitate size for the peak strengthening. Nevertheless, this aging temperature falls within the 300–600°C embrittlement regime and can result in a low impact toughness as in the HSLA-100 steel. Kong *et al.* [82] strived to solve this strength-impact toughness paradox. They decreased the Cu content from the previously 2 wt% in Jiao and Liu's work to only 1.3wt% for reducing the embrittlement and a further cost reduction. The authors reported a successful realization of GPa-grade nanostructured steels (YS and UTS over 1000 MPa, tensile ductility more than 10%) through a simple and short 10-min heat treatment at 640°C, avoiding the 300–600°C embrittlement regime

after the 900°C solution treatment. They discovered that the realization of GPa-grade nanostructured steels even after annealing at 640°C is due to the multiple strength- ening mechanisms. The additions of Cu, Ni, and C can stabilize the FCC phase at high temperatures (e.g.,~900°C) and give multiple complex strengthening mechanisms at lower temperatures (<700°C), depending on the cooling rate and heat treatment conditions. The strengthening mixtures of the nanostructured steels with different heat treatment schedules are presented in Fig. 9. Moreover, their impact results also suggest that the embrittlement of the nanostructured steels could be at- tributed to the segregation of impurities along the prior austenite grain boundaries. As the temperature passed through the embrittlement regime during slow cooling or aging, the impurities segregated into the prior austenite grain boundaries, weakening the prior austenite grain boundaries, and thus resulted in a very low impact toughness (<50 J at −20°C) accompanied with the intergranular fracture, as shown in Fig. 10. The nano- structured steels regained their impact toughness (~200 J even at −40°C) after water quenching from the 900°C solution treatment followed by aging at temperatures above the embrittlement regime (>600°C) with a subsequent fast quenching. The fast quenching is the key to the improved impact toughness of the steels. The impurities boiled off from the prior austenite grain boundaries during the high temperature (>600°C) aging. The subsequent rapid cooling (such as water quenching) froze the impurities from segregating back to the prior austenite grain boundaries, and hence improved the impact toughness. By optimizing the heat treatment condition, the authors believed the nanostructured steels can obtain their strengths over 1 GPa with a good tensile ductility over 10% and superior low temperature (−40°C) impact toughness over 200 J. These properties allow the nanostructured steels to possess strengths and impact toughness more superior than the X80 steel (YS ~550 MPa, UTS ~750 MPa, impact toughness ~200 J at −40°C [83]) used in the recent West-East

gas pipelines spanning over 5000 km across China. As indicated in Fig. 10, the nanostructured steels failed through a mixed brittle intergranular-cleavage mechanism. There might be other factors, apart from the impurities segregating along the prior austenite grain boundaries during slow cooling, possibly contributing to the low impact toughness of the nanostructured steels [84].

NANOSCALE Cu AND NiAl PRECIPITATIONS IN NANOSTRUCTURED STEELS

The nano-precipitates of the advanced nanostructured steels are metastable and maintain a very high coherency with the BCC steel matrix [7]. For instance, the Cu-rich nano-precipitates are ultrafine (<4nm in diameter) and have the BCC structure during the initial stage of nucleation[5,10,85]. As the aging proceeds, they grow larger (>4nm) and transform martensitically [86,87] into the semi-coherent 9R structure before turning into the incoherent FCC structure (>37 nm)[85,88,89]. Deformation-induced BCC to 9R martensitic transformation was also reported [90,91]. Meanwhile, the NiAl nanoprecipitates have the B2 structure[7] and they keep the same structure even after growing into a size as large as 200 nm in diameter[63]. These Cu-rich and NiAl nanoprecipitates have a spherical morphology in the initial stage of aging. With a prolonged aging, they start to lose their coherency and grow longitudinally, revealing a rod- like [9,10] or cuboidal shape [13,92].

The origin of the Cu-rich nano-precipitation lies behind the limited solubility (only ~0.15 wt% at 550°C) of Cu solutes in the BCC Fe solid solution [93,94] and the positive enthalpy of mixing between the Fe and Cu atoms [95]. Once cooled down from the homogenization temperature, a solid solution supersaturated with Cu solutes is created and this drives the nucleation of Cu-rich precipitates. Kolli and Seidman [10] performed a comprehensive study on the composition evolution of the Cu-rich nano-precipitates. At the beginning of the aging process, the core of the ultrafine BCC metastable Cu-rich

nano-precipitates contains a significant level of Fe (~30 to 40 at%), Ni (~8 at%), Al (~6at%), and Mn (~1.5 at%). The authors suggested that these elements are important in stabilizing the metastable BCC Cu-rich nanoprecipitates. Similar observations were also reported by Kapoor *et al*. [9] and Jiao *et al*. [94]. Isheim's work [96] on nanostructured steels containing a very low level of Ni (0.82 wt%) and Al (0.03 wt%) also reported strong Fe (33 at%) and Al (0.5 at%) enrichments in the BCC Cu-rich core. Nevertheless, there were also cases where pure BCC Cu core without the enrichment of alloying elements reported in[5,97–99]. Zhu *et al*.[100] performed a phase field modelling on the Cu precipitation in the Fe-Cu alloy system. Their work suggested that the compo- sition of the Cu core at the early stages of precipitation depends on the alloy composition and the aging temperature.

As the Cu-rich precipitates grow and transform into the thermodynamically stable FCC structure, more Cu atoms enter the precipitates' core while Fe atoms are rejected out [9]. The Ni, Mn, and Al atoms show a complex be–havior. These elements enter the core at the early stages of precipitation and their concentration decreases with further aging [10]. Liu *et al*. [101] reported that Mn is more readily to retain in the core as compared with Ni. Jiao *et al*. [5] pointed out that the presence of Ni in the Cu-rich core is very important as it can encourage the Cu-rich precipitation by reducing the strain energy nucleation barrier. Many studies showed that the Cu-rich nano-precipitate/matrix interface is wet by diffuse layers or non-uniform shells of Ni, Mn, and Al [9,10,95,96]. The enrichment of these elements at the interface can come from the solute rejection of both the Cu-rich core and matrix. Isheim *et al*. [96] pointed out that the elemental segregation is attributed to a thermodynamic driving force, for instance to reduce the interfacial energy that further helps promote the Cu-rich precipitation, and not a consequence of the solute pile-up. The segregation of Ni and Mn can be attributed to the positive mixing enthalpy (repulsive interaction) with Cu while that of Al to the large negative mixing

enthalpy (attractive interaction) with Ni and Mn [5,95]. As the aging process goes on, the elemental segregation becomes more pronounced and the ordered B2-NiAl phase starts to nucleate and grow heterogeneously at the precipitate/matrix interface, side-byside with the Cu-rich precipitates, forming Cu/NiAl coprecipitates [9,10,94,102]. The NiAl precipitation arises from the miscibility gap between the ordered B2-NiAl phase and the disordered BCC Fe in the Fe-Al-Ni alloy system [32]. The NiAl phase has a higher solubility in the BCC Fe than the Cu atoms [94]. A minimum 2.5 wt% of Ni and 1 wt% of Al are needed for a successful NiAl precipitation from the BCC Fe [22,94]. The metastable NiAl precipitates are not purely Ni and Al atoms but contain Cu, Mn, Fe atoms for reducing the lattice misfit strain and thus enhanced precipitation [7,8,94].

According to Jiao *et al*. [94], these Cu-rich and NiAl nanoprecipitates can nucleate independently and their precipitation sequence is strongly related to the relative amounts of Cu, Ni, and Al. In nanostructured steels containing high-Cu and low-Ni/Al, Cu-rich precipitates will first come out from the supersaturated solid solution followed by the rejection of Ni and Al atoms to the surrounding precipitate/matrix interphases. The reversed is true for the nanostructured steels containing low-Cu and high-Ni/Al. The detailed precipitation sequence of the Cu-rich and NiAl precipitates is summarized in Fig. 11 [92]. Xu *et al*. [103] in Zhang's group also discovered that the additions of Mo can reduce the diffusion coefficient of Cu, Ni, and Al atoms and subsequently modify the precipitation sequence of these precipitates.

PRECIPITATE-DISLOCATION INTERACTIONS AND THE STRENGTH- DUCTILITY PARADOX

The strength and ductility (or toughness) of the nanostructured steels strengthened by a high

number density of ultrafine coherent precipitates show a very intriguing behavior. The conventional wisdom taught us that the shearing of coherent precipitates produces a localized slip and deteriorates the ductility significantly [39,104,105]. Dislocation looping around non-deformable semi or incoherent particles is more favorable for improved ducti- lity as the slip distribution is more refined and homogenized.

The extremely low room-temperature bending ductility (<1%) of the NiAl precipitate-strengthened nano- structured steel (FBB-8) developed by Liaw's group[54] seems to agree with the conventional wisdom. As discussed in the previous sections, the FBB-8 steel contains duplex-type NiAl precipitates: the relatively large (~100nm in diameter) primary NiAl precipitates and the ultrafine (~3nm in diameter) secondary NiAl precipitates. Sun *et al.*[54] argued that the brittleness could be ascribed to the ultrafine NiAl precipitates. First, the ultrafine NiAl precipitates could have excessively hardened the steel matrix, resulting in YS higher than the fracture strength of the NiAl precipitates. The NiAl pre- cipitates thus served as crack initiation sites and the cracks could propagate through the steel matrix easily due to the excessive hardening, as shown in Fig. 12. Secondly, the ultrafine NiAl precipitates could also create stress inhomogeneity due to slip localization, in agreement with the conventional wisdom. Stallybrass *et al.* [32] also supported that the ultrafine precipitates can lead to reduced ductility due to the restricted dislocation motion in the matrix, as a consequence of reduced interparticle spacing. However, a careful observation on Fig. 12 reveals that the cracks were actually formed at the large primary NiAl precipitates. Cracks might not have initiated at the ultrafine secondary NiAl precipitates. The dispersion of ultrafine precipitates can restrict the dislocation motion to form a stress concentration and thus raise the stress required for crack nucleation [104]. The brittleness can be a consequence of the easy crack nucleation due to the large

primary precipitates. Large precipitates often facilitate a stress concentration and promote the nucleation of cracks [106]. Once the cracks are nucleated at large primary NiAl precipitates, the cracks propagate easily through the fine dispersion of secondary NiAl precipitates without losing energy [104]. Apart from the size and interparticle spacing, the high-volume fraction of NiAl precipitates and the increased Al content in the steel matrix can also contribute to the br ittleness [63,107].

On the other hand, the studies from Jiao *et al*.[5–7], Zhang *et al*. [11,14], Jiang *et al*. [8], Kapoor *et al*.[108] and Vaynman *et al*.[35] formed another school of thoughts. Their studies suggest that the ultrafine dispersion of high-number-density coherent precipitates can improve strength dramatically with almost no compromise of ductility, breaking the strength-ductility convention. Jiang *et al*.[8] attributed the ductility enhancement to the stress homogenization due to the ultrafine dispersion of high-number-density coherent precipitates. The high coherency between the precipitate and matrix reduces the strain accumulation and prevents crack initiation as the dislocations shear through the precipitates. Zhang *et al*.[11] also pointed out the local disordering of the NiAl precipitates due to their off-stoichiometric composition[109] and the highly coherent precipitates allow dislocations to shear through easily without a significant change of their Burger's vector[105]. Kapoor *et al*.[108] suggested the coherent precipitates can serve as a misfit center that encourages the formation of mobile kink segments, helping the dislocations to move out from the Peierls valley easily [110]. The recent *in-situ* neutron diffraction analyses from Zhang's group [14] also revealed that the fine dispersion of nanoscale coherent precipitates can encourage simultaneous rotation of multiple crystal planes during deformation, leading to a better stress transfer and therefore enhanced ductility.

CURRENT LIMITATION AND FUTURE DEVELOPMENT

For the widespread use of the low-carbon advanced nanostructured steels in various engineering applications, the cost is always a main concern. The new advanced nanostructured steels must be cost-competitive in order to attract better market volume. This can be achieved by optimizing the steel chemistry, for example, by sub- stituting the expensive elements such as nickel (Ni) and molybdenum (Mo) with cheaper elements. Carbon is a potent and cost-effective solid solution strengthener in steels [111]. However, an addition of too much carbon will reduce the toughness of the steels. A thorough study on the effects of carbon on the mechanical properties of nanostructured steels is needed. Despite the successful development of ductile advanced nanostructured steels with tensile strengths approaching 2 GPa, there is still plenty of room for strength improvement as heavily cold drawn pearlitic wires can achieve tensile strengths as high as 7 GPa [112,113]. Most of the recent nanostructured steels are developed based on the dislocation shearing mechanism. Dislocation looping is another strengthening mechanism that can lead to a strength improvement. The looping mechanism was observed in steels strengthened with a relatively low number density (~10^{20} m^{-3}) and large non-deformable NiAl precipitates (~50 nm) [54]. The possibilities of obtaining strong yet ductile nanostructured steels by incorporating both mechanisms remain unknown. Alloying the nanostructured steels with appropriate Mn additions is another cheap yet effective solution for an enhanced strength-ductility balance as discussed in the text earlier. It is widely recognized that the Mn additions can stabilize the austenite phase. The austenite phase undergoes a gradual martensitic transformation during deformation and contributes to an enhanced ductility through a progressive TRIP effect. It was also reported by Raabe and co-workers [114,115] that the Mn additions can lead to the formation of linear complexions through the Mn segregation confined at the dislocation cores. By altering the chemistry and structure of these linear complexions, it is possible to control the mobility

of the dislocations and thereby provide a new approach to the development of nanostructured steels with an improved strength-ductility balance [116]. A si- milar ductilizing mechanism through manipulating the elemental segregation to form disordered nanolayers at the grain boundaries of the conventionally brittle long-range-ordered superlattice alloys was also demonstrated by Yang *et al.* [117] recently.

The embrittlement of nanostructured steels is still not fully resolved at the present time. The nanostructured steels can achieve an excellent impact toughness (~200 J) even at low temperatures (−40°C) while maintaining their room temperature YS at around 1 GPa by annealing beyond the embrittlement regime (300–600°C) followed by fast quenching. However, more work is still needed as the nanostructured steels with a higher YS are generally required to be annealed at temperatures (400–550°C) within the embrittlement regime. In applications that require service temperatures between 300–600°C, the nanostructured steels will still face the embrittlement problem as embrittling elements segregate back into the prior-austenite grain boundaries. Besides, the embrittling elements will also have a chance to get into the prior-austenite grain boundaries during the cooling stage after welding, especially in thick samples, reducing the impact toughness of the steels. One possible way to alleviate this problem will be adding boron (B) into the steels. Boron can delay the embrittlement by segregating into the prioraustenite grain boundaries during high temperature quenching through non-equilibrium segregation [118]. The segregation of B at the prior-austenite grain boundaries will reduce the interfacial energy and thus decrease the segregation of embrittling elements. Another possible way will be the design of steel chemistry so that a soft austenite phase exists, but at the expense of the steel strength generally [65,81,119–123]. Steels with ultrafine grains are also expected to demonstrate improved toughness as the dislocation pile-up and

crack propagation become more difficult, in addition to the reduced segregation of embrittling elements at grain boundaries [124–127]. Controlling the structure of the grain boundaries through grain-boundary engineering can also help in minimizing the segregation of embrittling elements[120,128,129]. Recent studies also suggest a more relaxed grain boundary structure[130–132] and the presence of intergranular amorphous film[133,134] are beneficial to toughness improvement. Heterogeneous columnar-type grains were also reported to be effective in suppressing crack propagation [135].

Weldability is another important issue when it comes to the real applications of nanostructured steels. The advanced nanostructured steels contain low-carbon and display superior weldability without causing any cracks [19]. However, the nanostructured steels often experience precipitate dissolution in the fusion zone during the welding process, leading to joint softening. A post-weld heat treatment is required to recover the strength of the joint and this translates into an additional cost. Based on the welding experiment by Jiao *et al.*[19], a simple post weld heat treatment at 600°C for 30min can successfully recover the YS of the Cu/NiAl co-precipitate-strength-ened low-carbon nanostructured steel from 790MPa in the as-weld condition to 1460MPa (by 87%) with satisfactory ductility. On the other hand, the development of a unique welding technique that minimizes the microstructural damage without the need of post-weld heat treatments is also highly desirable, especially important for large-scale infrastructures and future advanced nanostructured steels with thinner gauges. In line with this, Chen *et al*. [20] demonstrated that the nanostructured steels with the combined Cu and Mn additions show excellent weldability with satisfactory strength and ductility through a magnetic field-assisted laser welding without the subsequent post-weld heat treatments. Moreover, due to the low precipitate dissolution temperature, the nanostructured steels show a limited creep resistance in applications with service temperatures above 700°C [69]. By incorporating

misfit strains at the pre- cipitate/matrix interface, it is possible to enhance the creep resistance to even comparable to the Haynes 282 Ni-based superalloys [69]. It is also very intriguing to note that the grain boundaries decorated with multi-elemental segregation display an exceptional resistance to coarsening even at high temperatures [117]. Coherent boundaries are also known to exhibit extraordinary thermal stability [136–138], and all of these can open up new opportunities for the development of high-temperature steels.

CONCLUSION

In essence, the recently developed high-strength steels rely heavily on a high level of carbon additions which often lead to inferior weldability. This paper reviews the recent development of low-carbon advanced nanostructured steels strengthened by coherent Cu-rich and NiAl nano-precipitates. These advanced nanostructured steels possess a low production cost, excellent strength-ductility balance, superior weldability, good fabricability, and high impact toughness even at a temperature as low as −40°C; thus, they are well suited for various engineering applications. An exceptional strength-ductility balance can be obtained by adding Mn for the formation of complex heterogeneous multiphase grain structures with ultrafine coherent nano-precipitates. The development of strong (YS >2 GPa) yet ductile (tensile elongation to 10%) and low-cost advanced nanostructured steels with a good weldability that can potentially serve in both high temperature (>700°C) and cryogenic (<−40°C) applications for the steel industry will be the focus on the future research direction.

References

1. Bhadeshia HKDH. The first bulk nanostructured metal. Sci Tech Adv Mater, 2013, 14: 014202

2. Miller RL. Ultrafine-grained microstructures and mechanical properties of alloy steels. Metall

Trans, 1972, 3: 905–912.

3. Halfa H. Recent trends in producing ultrafine grained steels. J Min Mater Charact Eng, 2014, 02: 428–469.

4. Garcia-Mateo C, Caballero FG, Bhadeshia HKDH. Development of hard bainite. ISIJ Int, 2003, 43: 1238–1243.

5. Jiao ZB, Luan JH, Zhang ZW, *et al.* Synergistic effects of Cu and Ni on nanoscale precipitation and mechanical properties of high- strength steels. Acta Mater, 2013, 61: 5996–6005.

6. Jiao ZB, Luan JH, Miller MK, *et al.* Precipitation mechanism and mechanical properties of an ultra-high strength steel hardened by nanoscale NiAl and Cu particles. Acta Mater, 2015, 97: 58–67.

7. Jiao ZB, Luan JH, Miller MK, *et al.* Effects of Mn partitioning on nanoscale precipitation and mechanical properties of ferritic steels strengthened by NiAl nanoparticles. Acta Mater, 2015, 84: 283–291.

8. Jiang S, Wang H, Wu Y, *et al.* Ultrastrong steel *via* minimal lattice misfit and high-density nanoprecipitation. Nature, 2017, 544: 460–464.

9. Kapoor M, Isheim D, Ghosh G, *et al.* Aging characteristics and mechanical properties of 1600MPa body-centered cubic Cu and B2-NiAl precipitation-strengthened ferritic steel. Acta Mater, 2014, 73: 56–74.

10. Kolli RP, Seidman DN. The temporal evolution of the decom- position of a concentrated multicomponent Fe–Cu-based steel. Acta Mater, 2008, 56: 2073–2088.

11. Zhang Z, Liu CT, Miller MK, *et al.* A nanoscale co-precipitation approach for property enhancement of Fe-base alloys. Sci Rep, 2013, 3: 1327.

12. Gagliano MS, Fine ME. Characterization of the nucleation and growth behavior of copper

precipitates in low-carbon steels. Metall Mat Trans A, 2004, 35: 2323–2329.

13. Jiao ZB, Luan JH, Miller MK, *et al.* Co-precipitation of nanoscale particles in steels with ultra-high strength for a new era. Mater Today, 2017, 20: 142–154.

14. Xu SS, Li JP, Cui Y, *et al.* Mechanical properties and deformation mechanisms of a novel austenite-martensite dual phase steel. Int J Plast, 2020, 128: 102677.

15. Zhou BC, Yang T, Zhou G, *et al.* Mechanisms for suppressing discontinuous precipitation and improving mechanical properties of NiAl-strengthened steels through nanoscale Cu partitioning. Acta Mater, 2021, 205: 116561.

16. Li Y, Li W, Xu C, *et al.* Investigation of hierarchical precipitation on bimodal-grained austenite and mechanical properties in quenching-partitioning-tempering steel. Mater Sci Eng-A, 2020, 781: 139207.

17. Li Y, Li W, Min N, *et al.* Homogeneous elasto-plastic deformation and improved strain compatibility between austenite and ferrite in a co-precipitation hardened medium Mn steel with enhanced hydrogen embrittlement resistance. Int J Plast, 2020, 133: 102805.

18. Kong HJ, Yang T, Chen R, *et al.* Breaking the strength-ductility paradox in advanced nanostructured Fe-based alloys through combined Cu and Mn additions. Scripta Mater, 2020,186:213– 218.

19. Jiao ZB, Luan JH, Guo W, *et al.* Effects of welding and post-weld heat treatments on nanoscale precipitation and mechanical properties of an ultra-high strength steel hardened by NiAl and Cu nanoparticles. Acta Mater, 2016, 120: 216–227.

20. Chen R, Kong HJ, Luan JH, *et al.* Effect of external applied magnetic field on microstructures and mechanical properties of laser welding joint of medium-Mn nanostructured steel. Mater Sci Eng-

A, 2020, 792: 139787.

21. Isheim D, Kolli RP, Fine ME, *et al.* An atom-probe tomographic study of the temporal evolution of the nanostructure of Fe–Cu based high-strength low-carbon steels. Scripta Mater, 2006, 55: 35–40.

22. Jiao ZB, Luan JH, Zhang ZW, *et al.* High-strength steels hardened mainly by nanoscale NiAl precipitates. Scripta Mater, 2014, 87: 45–48.

23. Zhang ZW, Liu CT, Wang XL, *et al.* Effects of proton irradiation on nanocluster precipitation in ferritic steel containing fcc al- loying additions. Acta Mater, 2012, 60: 3034–3046.

24. Busby J. NEET-Nuclear Energy Enabling Technologies Reactor Materials. News for the reactor materials crosscut. US Depart- ment of Energy, May 2015. [Online]. Available at: https://www.energy.gov/sites/prod/files/2015/08/f25/NEET-Reactor%20Mate-rials%20Newsletter%20-%20Issue%201.pdf.

25. Vaynman S, Fine ME, Ghosh G, *et al*. Copper precipitation hardened, high strength, weldable steels. In: The Proceedings of the 4th Materials Engineering Conference: Materials for the New Millennium. Washington, 1996, 10–14.

26. Liu Q, Liu W, Xiong X. Correlation of Cu precipitation with austenite-ferrite transformation in a continuously cooled multicomponent steel: An atom probe tomography study. J Mater Res, 2012, 27: 1060–1067.

27. World Steel Association. Future steel vehicle results and reports & cost model. World Auto Steel, Feb 2020. [Online]. Available: https://www.worldautosteel.org/projects/future-steel-vehicle/ phase-2-results/.

28. Roland F, Manzon L, Kujala P, *et al*. Advanced joining techniques in European shipbuilding. J Ship Prod, 2004, 20: 200–210.

29. He BB, Hu B, Yen HW, *et al.* High dislocation density-induced large ductility in deformed and partitioned steels. Science, 2017, 357: 1029–1032.

30 Liu L, Yu Q, Wang Z, *et al.* Making ultrastrong steel tough by grain-boundary delamination. Science, 2020, 368: 1347–1352.

31. Raabe D, Ponge D, Dmitrieva O, *et al.* Nanoprecipitate-hardened 1.5 GPa steels with unexpected high ductility. Scripta Mater, 2009, 60: 1141–1144.

32. Stallybrass C, Schneider A, Sauthoff G. The strengthening effect of (Ni,Fe)Al precipitates on the mechanical properties at high temperatures of ferritic Fe–Al–Ni–Cr alloys. Intermetallics, 2005, 13: 1263–1268.

33. Vaynman S, Fine ME, Bhat SP. High strength copper steel for rail tank cars to bridges. Copper Development Association Inc., De-cember 2006. [Online]. Available: https://www.copper.org/publications/newsletters/innovations/2006/12/high_strength_cu_steel.html

34. Vaynman S, Fine ME, Chung YW. Super-tough steel for bridges and other applications. Center for the Commercialization of In- novative Transportation Technology, USDOT University Transportation Center, 2009.

35. Vaynman S, Isheim D, Prakash Kolli R, *et al.* High-strength low- carbon ferritic steel containing Cu-Fe-Ni-Al-Mn precipitates. Metall Mat Trans A, 2008, 39: 363–373.

36. Kolli RP, Seidman DN. Heat treatment of copper precipitation- strengthened steels. In: Dossett JL, Totten GE. ASM Handbook. Volume 4D. Heat Treating of Irons and Steels. Phoenix: ASM International, 2014. 188–203.

37 ine M, Vaynman S. Monitoring and advising on Lave Villa Bridge. Northwestern University Libraries, 2007.

38 Kolli RP, Seidman DN. Co-precipitated and collocated carbides and Cu-rich precipitates in a Fe-Cu steel characterized by atom- probe tomography. Microsc Microanal, 2014, 20: 1727–1739.

39. Martin JW. Precipitation Hardening. Oxford: Butterworth- Heinemann, 1998.

40 Klamecki B. Chapter 19: Cold-working process. University of Minnesota, 2002. [Online]. Available: http://www.menet.umn. edu/~klamecki/degarmo/.

41. Bhadeshia HKDH. TRIP-assisted steels? ISIJ Int, 2002, 42: 1059– 1060.

42. Marquis EA, Choi PP, Danoix F, *et al.* New insights into the atomic-scale structures and behavior of steels. Micros Today, 2012, 20: 44–48.

43. Ryu JH, Kim DI, Kim HS, *et al.* Strain partitioning and me- chanical stability of retained austenite. Scripta Mater, 2010, 63: 297–299.

44. Zhu YT, Wu XL. Ductility and plasticity of nanostructured me- tals: Differences and issues. Mater Today Nano, 2018, 2: 15–20.

45. Yang MX, Yuan FP, Xie QG, *et al.* Strain hardening in Fe-16Mn- 10Al-0.86C-5Ni high specific strength steel. Acta Mater, 2016, 109: 213–222.

46. Lee S, Lee SJ, De Cooman BC. Work hardening behavior of ultrafine-grained Mn transformation-induced plasticity steel. Acta Mater, 2011, 59: 7546–7553.

47. Sun B, Fazeli F, Scott C, *et al.* Critical role of strain partitioning and deformation twinning on cracking phenomenon occurring during cold rolling of two duplex medium manganese steels. Scripta Mater, 2017, 130: 49–53.

48. Liu XL, Xue QQ, Wang W, *et al.* Back-stress-induced strength- ening and strain hardening in dual-phase steel. Materialia, 2019, 7: 100376.

49. Wu X, Zhu Y. Heterogeneous materials: A new class of materials with unprecedented mechanical

properties. Mater Res Lett, 2017, 5: 527–532.

50 .Lu K. Making strong nanomaterials ductile with gradients. Sci- ence, 2014, 345: 1455–1456.

51. Wu XL, Jiang P, Chen L, *et al.* Synergetic strengthening by gra- dient structure. Mater Res Lett, 2014, 2: 185–191.

52. Tan X, Ponge D, Lu W, *et al.* Joint investigation of strain parti- tioning and chemical partitioning in ferrite-containing TRIP- assisted steels. Acta Mater, 2020, 186: 374–388.

53. Tan X, Ponge D, Lu W, *et al.* Carbon and strain partitioning in a quenched and partitioned steel containing ferrite. Acta Mater, 2019, 165: 561–576.

54. Sun Z, Song G, Ilavsky J, *et al.* Duplex precipitates and their effects on the room-temperature fracture behaviour of a NiAl- strengthened ferritic alloy. Mater Res Lett, 2015, 3: 128–134.

55. Seetharaman V, Sundararaman M, Krishnan R. Precipitation hardening in a PH 13-8 Mo stainless steel. Mater Sci Eng, 1981, 47: 1–11.

56. Taillard R, Pineau A, Thomas BJ. The precipitation of the in- termetallic compound NiAl in Fe-19 wt%Cr alloys. Mater Sci Eng, 1982, 54: 209–219.

57. Taillard R, Pineau A. Room temperature tensile properties of Fe-19 wt% Cr alloys precipitation hardened by the intermetallic compound NiAl. Mater Sci Eng, 1982, 56: 219–231.

58. Guo Z, Sha W, Vaumousse D. Microstructural evolution in a PH 13-8 stainless steel after ageing. Acta Mater, 2003, 51: 101–116.

59. Leitner H, Schober M, Schnitzer R. Splitting phenomenon in the precipitation evolution in an Fe-Ni-Al-Ti-Cr stainless steel. Acta Mater, 2010, 58: 1261–1269.

60. Niu M, Zhou G, Wang W, *et al.* Precipitate evolution and strengthening behavior during aging process in a 2.5 GPa grade maraging steel. Acta Mater, 2019, 179: 296–307.

61. Sun Z, Song G, Ilavsky J, *et al.* Nano-sized precipitate stability and its controlling factors in a NiAl-strengthened ferritic alloy. Sci Rep, 2015, 5: 16081.

62. Teng ZK, Miller MK, Ghosh G, *et al.* Characterization of nano- scale NiAl-type precipitates in a ferritic steel by electron micro- scopy and atom probe tomography. Scripta Mater, 2010, 63: 61– 64.

63. Teng ZK, Liu CT, Ghosh G, *et al.* Effects of Al on the micro- structure and ductility of NiAl-strengthened ferritic steels at room temperature. Intermetallics, 2010, 18: 1437–1443.

64. Erlach SD, Leitner H, Bischof M, *et al.* Comparison of NiAl precipitation in a medium carbon secondary hardening steel and C-free PH 13-8 maraging steel. Mater Sci Eng-A, 2006, 429: 96– 106.

65. Sha W, Leitner H, Guo Z, *et al*. Phase transformations in mara- ging steels. In: Pereloma E, Edmonds DV (Eds). Phase Trans- formations in Steels: Diffusionless Transformations, High Strength Steels, Modelling and Advanced Analytical Techniques. Volume 2 in Woodhead Publishing Series in Metals and Surface Engineering. Cambridge: Woodhead Publishing Limited, 2012. 332–362.

66. Sun L, Simm TH, Martin TL, *et al.* A novel ultra-high strength maraging steel with balanced ductility and creep resistance achieved by nanoscale β-NiAl and Laves phase precipitates. Acta Mater, 2018, 149: 285–301.

67. Hulme-Smith CN, Bhadeshia HKDH. Mechanical properties of thermally-stable, nanocrystalline bainitic steels. Mater Sci Eng-A, 2017, 700: 714–720.

68. Simm TH, Sun L, Galvin DR, *et al.* The effect of a two-stage heat- treatment on the microstructural and mechanical properties of a maraging steel. Materials, 2017, 10: 1346

69. Song G, Sun Z, Li L, *et al*. Ferritic alloys with extreme creep resistance *via* coherent hierarchical precipitates. Sci Rep, 2015, 5: 16327.

70. Teng ZK, Zhang F, Miller MK, *et al.* New NiAl-strengthened ferritic steels with balanced creep resistance and ductility de- signed by coupling thermodynamic calculations with focused experiments. Intermetallics, 2012, 29: 110–115.

71. Calderon HA, Fine ME, Weertman JR. Coarsening and mor- phology of β' particles in Fe-Ni-Al-Mo ferritic alloys. Metall Trans A, 1988, 19: 1135–1146.

72. Base Metals Investing—Prices, Mining Stocks and News. Glacier Media Group, Oct 2019. [Online]. Available: http://www.in- fomine.com/investment/base-metals/.

73. Pig Iron. SMM Information & Technology Co., Ltd., Oct 2019. [Online]. Available: https://price.metal.com/Pig-Iron .

74. Duan QQ, Qu RT, Zhang P, *et al.* Intrinsic impact toughness of relatively high strength alloys. Acta Mater, 2018, 142: 226–235.

75. Bandyopadhyay N, McMahon CJ. The micro-mechanisms of tempered martensite embrittlement in 4340-type steels. Metall Trans A, 1983, 14: 1313–1325.

76 .Basinski ZS, Christian JW. Mechanical properties of metals at low temperatures. In: Timmerhaus KD (Ed). Advances in Cryogenic Engineering. Advances in Cryogenic Engineering, vol 2. Boston: Springer, 1960.

77. Kwon KH, Yi IC, Ha Y, *et al.* Origin of intergranular fracture in martensitic 8Mn steel at cryogenic temperatures. Scripta Mater, 2013, 69: 420–423.

78. Horn RM, Ritchie RO. Mechanisms of tempered martensite embrittlement in low alloy steels. Metall Trans A, 1978, 9: 1039– 1053.

79. Seah MP. Interface adsorption, embrittlement and fracture in metallurgy. Surf Sci, 1975, 53: 168–212.

80. Dhua SK, Ray A, Sarma DS. Effect of tempering temperatures on the mechanical properties and microstructures of HSLA-100 type copper-bearing steels. Mater Sci Eng-A, 2001, 318: 197–210.

81. Liu Q, Wen H, Zhang H, *et al.* Effect of multistage heat treatment on microstructure and mechanical properties of high-strength low-alloy steel. Metall Mat Trans A, 2016, 47: 1960–1974.

82. Kong HJ, Xu C, Bu CC, *et al.* Hardening mechanisms and impact toughening of a high-strength steel containing low Ni and Cu additions. Acta Mater, 2019, 172: 150–160.

83. Shin SY, Hwang B, Lee S, *et al.* Correlation of microstructure and charpy impact properties in API X70 and X80 line-pipe steels. Mater Sci Eng-A, 2007, 458: 281–289.

84. Zhao Y, Tong X, Wei XH, *et al.* Effects of microstructure on crack resistance and low-temperature toughness of ultra-low carbon high strength steel. Int J Plast, 2019, 116: 203–215.

85. Han G, Xie ZJ, Li ZY, *et al.* Evolution of crystal structure of Cu precipitates in a low carbon steel. Mater Des, 2017, 135: 92–101.

86. Monzen R, Jenkins ML, Sutton AP. The bcc-to-9R martensitic transformation of Cu precipitates and the relaxation process of elastic strains in an Fe-Cu alloy. Philos Mag A, 2000, 80: 711–723.

87. Sun M, Zhang W, Liu Z, *et al.* Direct observations on the crystal structure evolution of nano Cu-precipitates in an extremely low carbon steel. Mater Lett, 2017, 187: 49–52.

88. Othen PJ, Jenkins ML, Smith GDW, *et al.* Transmission electron microscope investigations of the structure of copper precipitates in thermally-aged Fe–Cu and Fe–Cu–Ni. Philos Mag Lett, 1991, 64: 383–391.

89. Takahashi J, Kawakami K, Kobayashi Y. Consideration of parti- cle-strengthening mechanism of copper-precipitation-strength- ened steels by atom probe tomography analysis. Mater Sci Eng-A, 2012, 535: 144–152.

90. Lozano-Perez S, Jenkins ML, Titchmarsh JM. Evidence for de- formation-induced transformations of Cu-rich precipitates in an aged FeCu alloy. Philos Mag Lett, 2006, 86: 367–374.

91. Hu SY, Schmauder S, Chen LQ. Atomistic simulations of inter- actions between Cu precipitates and an edge dislocation in a BCC Fe single crystal. Phys Stat Sol B, 2000, 220: 845–846.

92. Sun Z. Microstructures and mechanical behavior of NiAl- strengthened ferritic alloys at room and elevated temperatures. Dissertation for the Doctoral Degree. Tennessee: University of Tennessee, 2015.

93. Liu CT, Jiao ZB, Luan JH. Copper-rich nanoclusters: Ferritic steels strengthened. In: Colás R, Totten GE (Eds). Encyclopedia of Iron, Steel, and Their Alloys. Florida: CRC Press, 2015. 875–886.

94. Jiao ZB, Luan JH, Miller MK, *et al.* Group precipitation and age hardening of nanostructured Fe-based alloys with ultra-high strengths. Sci Rep, 2016, 6: 21364.

95. Wen YR, Hirata A, Zhang ZW, *et al.* Microstructure characterization of Cu-rich nanoprecipitates in a Fe-2.5Cu-1.5Mn-4.0Ni- 1.0Al multicomponent ferritic alloy. Acta Mater, 2013, 61: 2133– 2147.

96. Isheim D, Gagliano MS, Fine ME, *et al.* Interfacial segregation at Cu-rich precipitates in a high-strength low-carbon steel studied on a sub-nanometer scale. Acta Mater, 2006, 54: 841–849.

97. Fine ME, Liu JZ, Asta MD. An unsolved mystery: The compo- sition of bcc Cu alloy precipitates in bcc Fe and steels. Mater Sci Eng-A, 2007, 463: 271–274.

98. Worrall GM, Buswell JT, English CA, *et al.* A study of the pre- cipitation of copper particles in a ferrite matrix. J Nucl Mater, 1987, 148: 107–114

99. Osamura K, Okuda H, Takashima M, *et al.* Small-angle neutron scattering study of phase decomposition in Fe-Cu binary alloy. Mater Trans JIM, 1993, 34: 305–311.

100. Zhu J, Zhang T, Yang Y, *et al.* Phase field study of the copper precipitation in Fe-Cu alloy. Acta

Mater, 2019, 166: 560–571.

101. Liu Q, Chen Y, Li C, *et al.* Compositional variants of Cu-rich precipitate in thermally aged ferritic steel. Acta Metall Sin (Engl Lett), 2018, 31: 465–470.

102. Kolli RP, Mao Z, Seidman DN, *et al.* Identification of a $Ni_{0.5}(Al_{0.5-x}Mn_x)B_2$ phase at the heterophase interfaces of Cu-rich precipitates in an α-Fe matrix. Appl Phys Lett, 2007, 91: 241903.

103. Xu SS, Liu YW, Zhang Y, *et al.* Precipitation kinetics and me- chanical properties of nanostructured steels with Mo additions. Mater Res Lett, 2020, 8: 187–194.

104. Martin JW. Micromechanisms in Particle-Hardened Alloys. Great Britian: Cambridge University Press, 1980

105. Hornbogen E, Zum Gahr KH. Distribution of plastic strain in alloys containing small particles. Metallography, 1975, 8: 181–202.

106. Baker I. Improving the ductility of intermetallic compounds by particle-induced slip homogenization. Scr Mater, 1999, 41: 109– 414.

107. Teng ZK, Liu CT, Miller MK, *et al.* Room temperature ductility of NiAl-strengthened ferritic steels: Effects of precipitate micro- structure. Mater Sci Eng-A, 2012, 541: 22–27.

108. Kapoor M, Isheim D, Vaynman S, *et al.* Effects of increased al- loying element content on NiAl-type precipitate formation, loading rate sensitivity, and ductility of Cu- and NiAl-precipita- tion-strengthened ferritic steels. Acta Mater, 2016, 104: 166–171.

109. Stoloff NS, Davies RG. The mechanical properties of ordered alloys. Prog Mater Sci, 1968, 13: 1–84.

110. Fine ME, Vaynman S, Isheim D, *et al.* A new paradigm for de- signing high-fracture-energy steels. Metall Mat Trans A, 2010, 41: 3318–3325.

111. Honeycombe RWK, Bhadeshia HKDH. Steels: Microstructure and Properties. London: Edward Arnold, 1995.

112. Li Y, Raabe D, Herbig M, *et al.* Segregation stabilizes nanocrys- talline bulk steel with near theoretical strength. Phys Rev Lett, 2014, 113: 106104.

113. Morris JW, Guo Z, Krenn CR, *et al.* Advances in physical me- tallurgy and processing of steels. The limits of strength and toughness in steel. ISIJ Int, 2001, 41: 599–611.

114. Kuzmina M, Herbig M, Ponge D, *et al.* Linear complexions: Confined chemical and structural states at dislocations. Science, 2015, 349: 1080–1083.

115. Kwiatkowski da Silva A, Leyson G, Kuzmina M, *et al.* Confined chemical and structural states at dislocations in Fe-9wt% Mn steels: A correlative TEM-atom probe study combined with multiscale modelling. Acta Mater, 2017, 124: 305–315.

116. Kaplan WD. The mechanism of crystal deformation. Science, 2015, 349: 1059–1060.

117. Yang T, Zhao YL, Li WP. Ultrahigh-strength and ductile super- lattice alloys with nanoscale disordered interfaces. Science, 2020, 369: 427–432.

118. Kuzmina M, Ponge D, Raabe D. Grain boundary segregation engineering and austenite reversion turn embrittlement into toughness: Example of a 9 wt% medium Mn steel. Acta Mater, 2015, 86: 182–192.

119. Kong H, Liu C. A review on nano-scale precipitation in steels. Technologies, 2018, 6: 36.

120. Raabe D, Herbig M, Sandlöbes S, *et al.* Grain boundary segre- gation engineering in metallic alloys: A pathway to the design of interfaces. Curr Opin Solid State Mater Sci, 2014, 18: 253–261.

121. Li DZ, Wei YH, Hou LF, *et al.* Effect of temperature on impact properties and microstructural evolution of twinning induced plasticity steel. Mater Sci Tech, 2012, 28: 303–310.

122. Sugimoto K, Srivastava AK. Microstructure and mechanical properties of a TRIP-aided martensitic steel. Metallogr Micro-struct Anal, 2015, 4: 344–354.

123 Zou Y, Xu YB, Wang G, *et al.* Improved strength-ductility-toughness balance of a precipitation-strengthened low-carbon medium-Mn steel by adopting intercritical annealing-tempering process. Mater Sci Eng-A, 2021, 802:140636.

124. Song R, Ponge D, Raabe D. Mechanical properties of an ultrafine grained C–Mn steel processed by warm deformation and an- nealing. Acta Mater, 2005, 53: 4881–4892.

125. Ishida K. Effect of grain size on grain boundary segregation. J Alloys Compd, 1996, 235: 244–249.

126. Hou W, Liu Q, Gu J. Improved impact toughness by multi-step heat treatment in a 1400 MPa low carbon precipitation- strengthened steel. Mater Sci Eng-A, 2020, 797: 140077.

127. Armstrong RW. Dislocation pile-ups, strength properties and fracturing. Rev Adv Mater Sci, 2017, 48: 1–12.

128. Lejček P, Hofmann S, Paidar V. Solute segregation and classifi- cation of [100] tilt grain boundaries in α-iron: Consequences for grain boundary engineering. Acta Mater, 2003, 51: 3951–3963.

129. Watanabe T. Grain boundary design and control for high tem- perature materials. Mater Sci Eng-A, 1993, 166: 11–28.

130. Jang D, Atzmon M. Grain-boundary relaxation and its effect on plasticity in nanocrystalline Fe. J Appl Phys, 2006, 99: 083504.

131. Rupert TJ, Trelewicz JR, Schuh CA. Grain boundary relaxation strengthening of nanocrystalline Ni-W alloys. J Mater Res, 2012, 27: 1285–1294.

132. Lu K, Lu L, Suresh S. Strengthening materials by engineering coherent internal boundaries at the nanoscale. Science, 2009, 324: 349–352.

133. Pan Z, Rupert TJ. Amorphous intergranular films as toughening structural features. Acta Mater, 2015, 89: 205–214.

134. Khalajhedayati A, Pan Z, Rupert TJ. Manipulating the interfacial structure of nanomaterials to achieve a unique combination of strength and ductility. Nat Commun, 2016, 7: 10802.

135. Cao BX, Kong HJ, Fan L, *et al.* Heterogenous columnar-grained high-entropy alloys produce exceptional resistance to inter- mediate-temperature intergranular embrittlement. Scripta Mater, 2021, 194: 113622.

136. Anderoglu O, Misra A, Wang H, *et al.* Thermal stability of sputtered Cu films with nanoscale growth twins. J Appl Phys, 2008, 103: 094322.

137. Zhang X, Misra A. Superior thermal stability of coherent twin boundaries in nanotwinned metals. Scripta Mater, 2012, 66: 860– 865.

138. Zhou X, Li XY, Lu K. Stabilizing nanograins in metals with grain boundary relaxation. Scripta Mater, 2020, 187: 345–349.

139. Tempelman E. Lightweight materials, lightweight design? In: Karana E, Pedgley O, Rognoli V (Eds). Materials Experience: Fundamentals of Materials and Design. Boston: Elsevier, 2014. 247–258.

140. Wen YR, Li YP, Hirata A, *et al.* Synergistic alloying effect on microstructural evolution and mechanical properties of Cu pre- cipitation-strengthened ferritic alloys. Acta Mater, 2013, 61: 7726–7740.

Figure captions

Figure 1 A comparison on the strength-ductility performances of the recently developed low-carbon advanced nanostructured steels with the conventional commercialized steels [5,6,8,9,11,13,14,18,139].

Figure 2 A schematic showing the processing route of the nano-precipitate-strengthened low-carbon advanced nanostructured steels through (a) isothermal aging, (b) multi-step heat treatment, and (c) inter-phase precipitation.

Figure 3 The tensile stress-strain curve of Jiao and Liu's nanostructured steel strengthened with nanoscale coherent Cu precipitates (Fe-0.75Ni-2Cu-0.75Mn-0.3Al-2.25Cr-1 Mo-0.25V-0.07Ti-0.3Si-0.01B-0.08C, wt%). The snippet view: (a) the dimples indicating ductile fracture; (b) the ferritic grains; (c) the Cu precipitates through the three-dimensional (3D) reconstruction of atom probe tomography (APT) analyses. Rep¬rinted with permission from Ref. [5]. Copyright 2013, Elsevier.

Figure 4 The tensile stress-strain curve of Cu precipitate-strengthened nanostructured steel containing 8 wt% of Mn additions (Fe-8Mn-1Ni- 2Cu-3Cr-1.1Si-0.8Mo-0.5Al-0.3Ti-0.11C-0.02B, wt%). The snippet views: (a, b) the multi-phase submicron-grains before test and after 5% deformation; (c, d) the phase map before test and after 5% deformation, indicating TRIP effect during deformation; (e) the nanoscale coherent Cu precipitates sitting along the grain boundaries through the 3D re- construction of APT analyses. F: ferrite; A: austenite; Red: face-centered cubic (FCC) phase; Blue: BCC phase; Orange: hexagonal close-packed phase. Reprinted with permission from Ref. [8]. Copyright 2020, Elsevier.

Figure 5 The tensile stress-strain curve of Jiao and Liu's Fe-5Ni-1Al-3Mn advanced nanostructured steel. A huge strength increment of 540 MPa was achieved without a significant loss of ductility due

to the ultrafine dispersion of high number density coherent NiAl nano-pre- cipitates after aging at 550°C for 2 h. The snippet views: (a) the ductile fracture; (b, c) the ferritic grains before and after the 550°C/2 h aging; (d) the NiAl precipitates through the 3D reconstruction of APT analyses. AQ: as quenched. Reprinted with permission from Ref. [7]. Copyright 2015, Elsevier.

Figure 6 The tensile stress-strain curve of Jiang and Lu's advanced nanostructured steel (Fe-18Ni-3Al-4Mo-0.8Nb-0.08C-0.01B) strength- ened with ultrafine dispersion of coherent NiAl nano-precipitates, as demonstrated in the snippet view. Both strength and uniform elongation were improved after aging, breaking the strength-ductility trade-off. Reprinted with permission from Ref. [8]. Copyright 2017, Springer Nature.

Figure 7 (a) Dark field transmission electron microscopy image and (b) schematic diagram showing the hierarchical B2-NiAl/$L2_1$-Ni_2TiAl pre- cipitates in Song and Liaw's nanostructured steel. Reprinted with permission from Ref. [69]. Copyright 2015, Springer Nature.

Figure 8 The strength-impact toughness paradox of the HSLA-100 steel. The steel achieves its peak strength after aging at 500°C but at the minimum toughness. The impact toughness restores with aging above 600°C but at the expense of strength [80].

Figure 9 The strengthening mix indicating multiple strengthening mechanisms of the advanced nanostructured steel containing Cu and Ni additions. The advanced steel is insensitive to heat treatment and can achieve YS above 1000 MPa. FM: fresh martensite; B: bainite; TM: tempered martensite; P: Cu precipitation; C: carbides; GR: grain re- finement; SS: solid solution; AC: air cool; WQ: water quench. Reprinted with permission from Ref. [82]. Copyright 2019, Elsevier.

Figure 10 The fractured surface of nanostructured steel containing Cu and Ni additions after aging at 600°C followed by air cooling, indicating mixed intergranular-cleavage brittle fracture.

Reprinted with permission from Ref. [82]. Copyright 2019, Elsevier.

Figure 11 The precipitation sequence of the Cu-rich, NiAl, and Cu/NiAl co-precipitates in the advanced nanostructured steel containing Ni, Al, and Cu additions. The upper sequence indicates Cu-rich precipitation comes before NiAl in the high-Cu and low-Ni/Al steel while the reverse is true in the low-Cu and high-Ni/Al steel. Reprinted with permission from Ref. [94]. Copyright 2016, Springer Nature.

Figure 12 Cracks formed at the large primary NiAl precipitates and propagated through the hardened matrix. The fractured surface is shown in the inset. C: cracks; P: crack propagation. Reprinted with permission from Ref. [54]. Copyright 2015, Taylor and Francis.

Fig 1

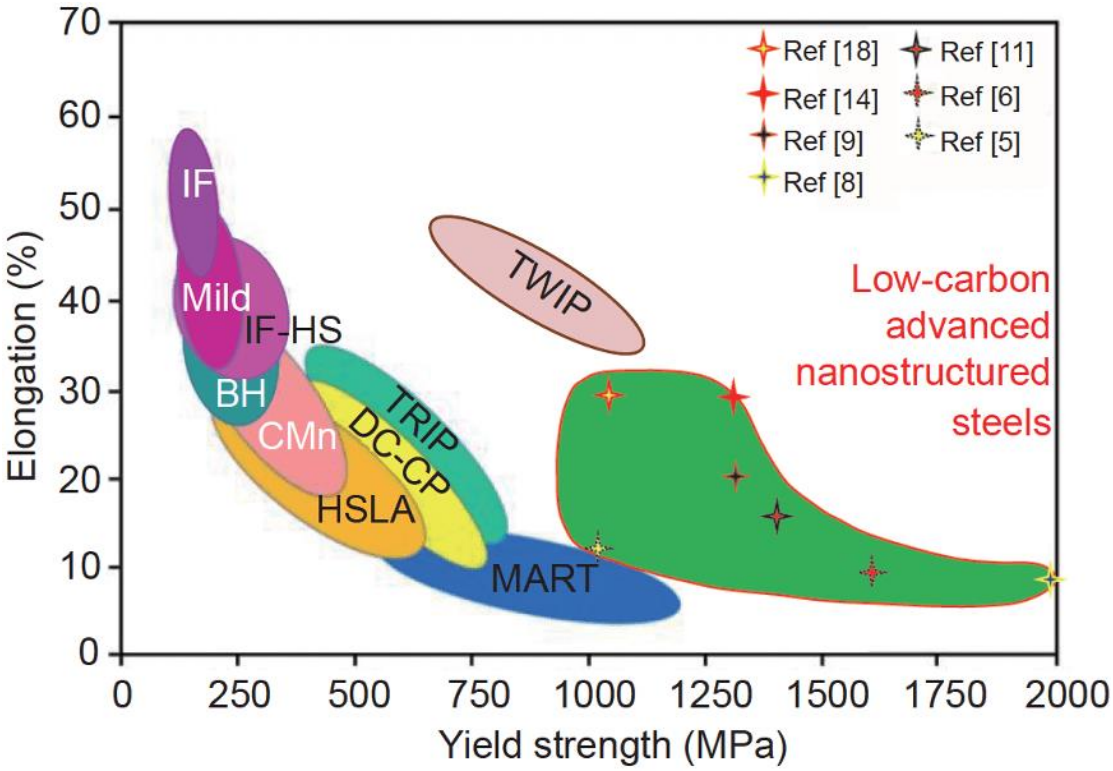
Ref [18]
Ref [14]
Ref [9]
Ref [8]
Ref [11]
Ref [6]
Ref [5]
IF
Mild
IF-HS
BH
CMn
HSLA
TRIP
DC-CP
MART
TWIP
Low-carbon
advanced
nanostructured
steels
Elongation (%)
Yield strength (MPa)
0
10
20
30
40
50
60
70
0
250
500
750
1000
1250
1500
1750
2000

Fig 2

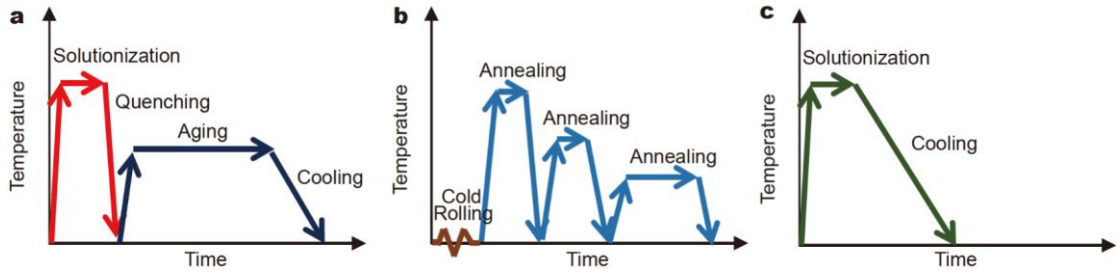
a
Solutionization
Quenching
Aging
Cooling
Temperature
Time
b
Annealing
Annealing
Annealing
Cold
Rolling
Temperature
Time
c
Solutionization
Cooling
Temperature
Time

Fig 3

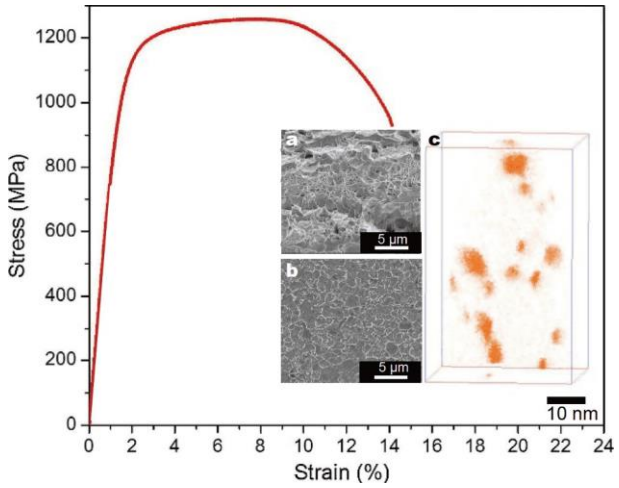

Fig 4

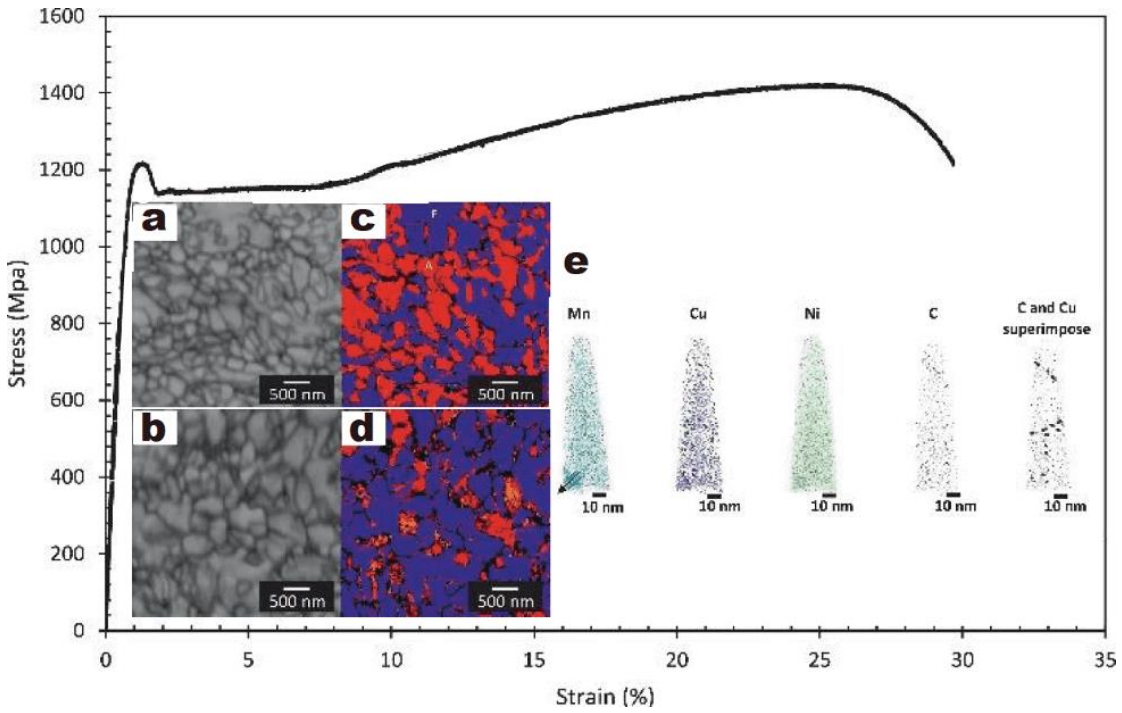
1600
1400
1200
1000
800
600
400
200
0
Stress (Mpa)
0
5
10
15
20
25
30
35
Strain (%)
a
b
c
d
e
500 nm
500 nm
500 nm
500 nm
Mn
Cu
Ni
C
C and Cu superimpose
10 nm
10 nm
10 nm
10 nm
10 nm

Fig 5

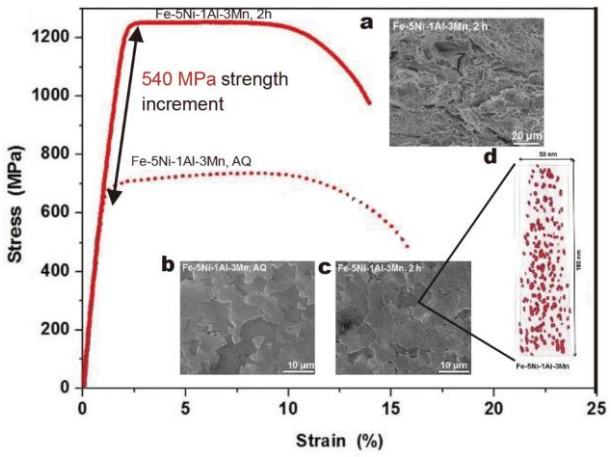
Fe-5Ni-1Al-3Mn, 2h
540 MPa strength increment
Fe-5Ni-1Al-3Mn, AQ
Stress (MPa)
Strain (%)
a
b
c
d
Fe-5Ni-1Al-3Mn, 2 h
Fe-5Ni-1Al-3Mn, AQ
20 μm
10 μm
10 μm
50 nm
180 nm
Fe-5Ni-1Al-3Mn

Fig 6

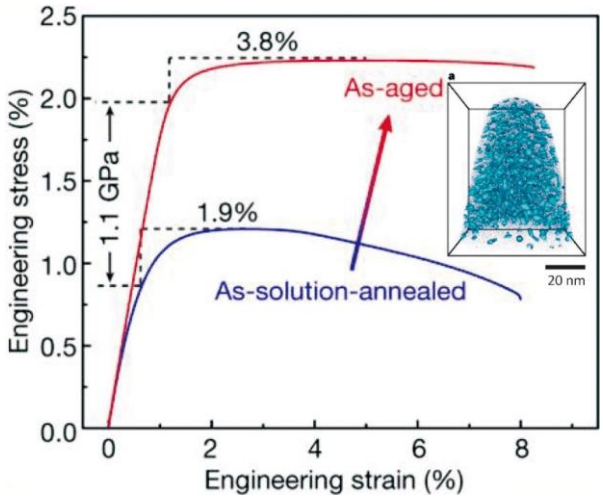
2.5
2.0
1.5
1.0
0.5
0.0
Engineering stress (%)
0
2
4
6
8
Engineering strain (%)
3.8%
1.9%
1.1 GPa
As-aged
As-solution-annealed
a
20 nm

Fig 7

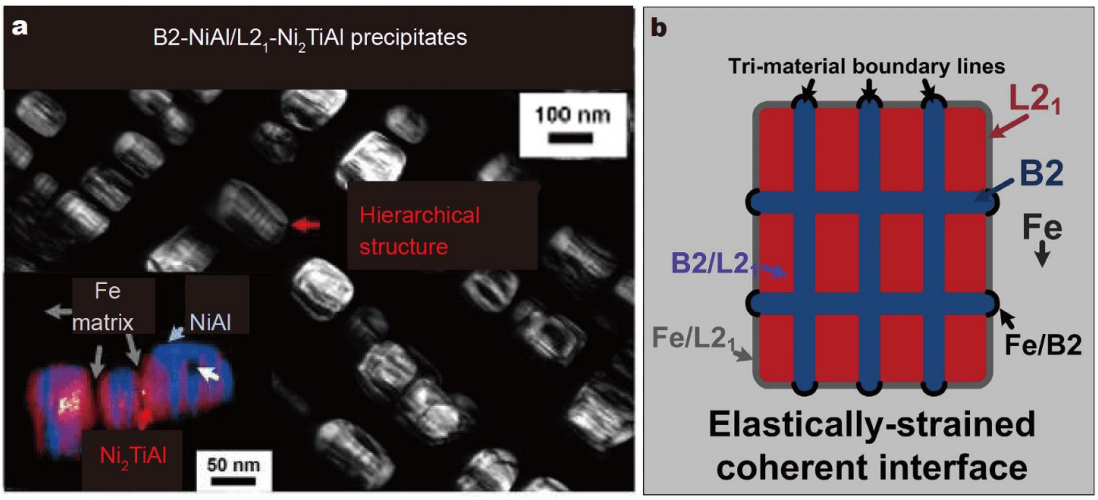
a
B2-NiAl/L2$_1$-Ni$_2$TiAl precipitates
100 nm
Hierarchical structure
Fe matrix
NiAl
Ni$_2$TiAl
50 nm
b
Tri-material boundary lines
L2$_1$
B2
Fe
B2/L2
Fe/L2$_1$
Fe/B2
Elastically-strained coherent interface

Fig 8

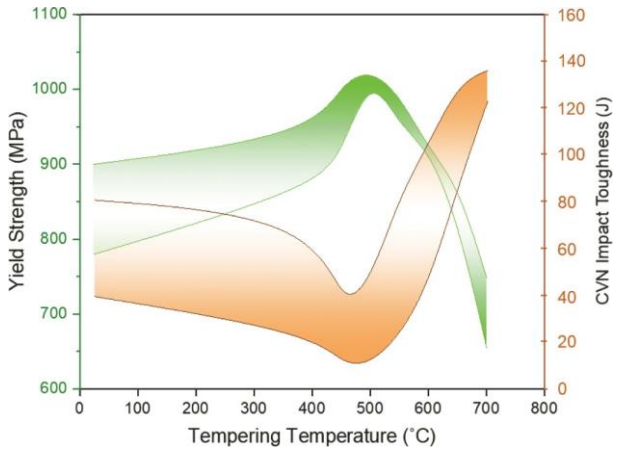
Yield Strength (MPa)
CVN Impact Toughness (J)
Tempering Temperature (°C)
1100
1000
900
800
700
600
160
140
120
100
80
60
40
20
0
0
100
200
300
400
500
600
700
800

Fig 9

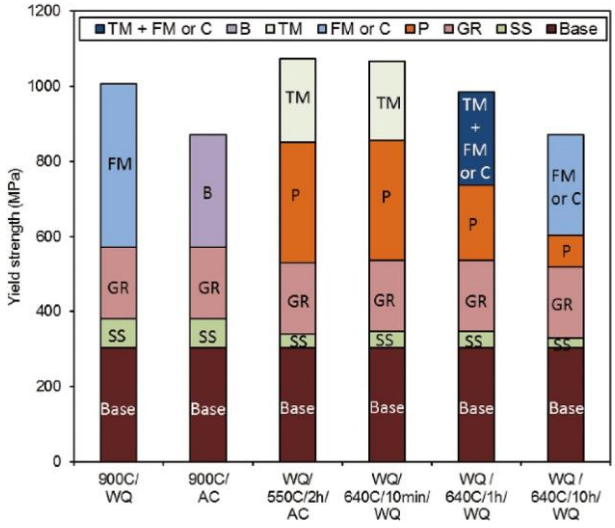
TM + FM or C
B
TM
FM or C
P
GR
SS
Base
Yield strength (MPa)
1200
1000
800
600
400
200
0
FM
GR
SS
Base
B
GR
SS
Base
TM
P
GR
SS
Base
TM
P
GR
SS
Base
TM + FM or C
P
GR
SS
Base
FM or C
P
GR
SS
Base
900C/ WQ
900C/ AC
WQ/ 550C/2h/ AC
WQ/ 640C/10min/ WQ
WQ / 640C/1h/ WQ
WQ / 640C/10h/ WQ

Fig 10

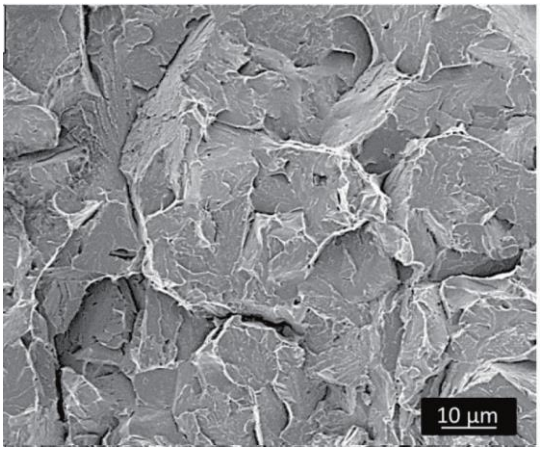

Fig 11

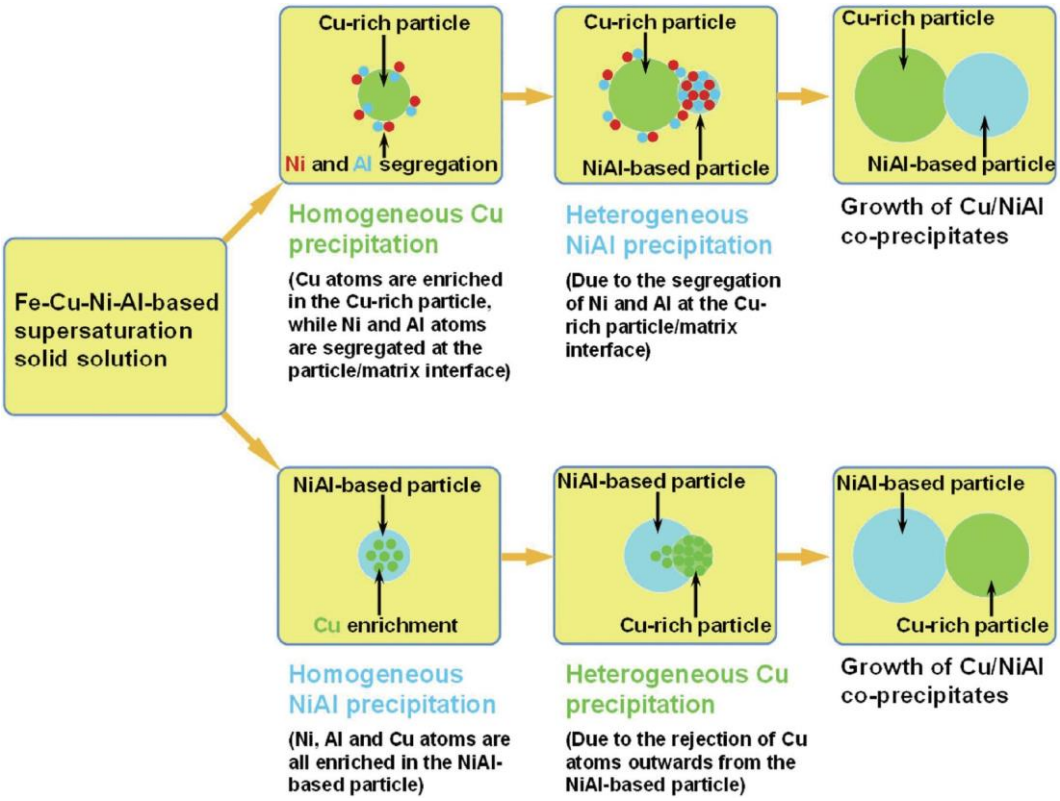
Fe-Cu-Ni-Al-based supersaturation solid solution
Cu-rich particle
Ni and Al segregation
Homogeneous Cu precipitation
(Cu atoms are enriched in the Cu-rich particle, while Ni and Al atoms are segregated at the particle/matrix interface)
Cu-rich particle
NiAl-based particle
Heterogeneous NiAl precipitation
(Due to the segregation of Ni and Al at the Cu-rich particle/matrix interface)
Cu-rich particle
NiAl-based particle
Growth of Cu/NiAl co-precipitates
NiAl-based particle
Cu enrichment
Homogeneous NiAl precipitation
(Ni, Al and Cu atoms are all enriched in the NiAl-based particle)
NiAl-based particle
Cu-rich particle
Heterogeneous Cu precipitation
(Due to the rejection of Cu atoms outwards from the NiAl-based particle)
NiAl-based particle
Cu-rich particle
Growth of Cu/NiAl co-precipitates

Fig 12